# Single-Shot Spectrometry for X-Ray Free-Electron Lasers

Makina Yabashi,[1,5,*] Jerome B. Hastings,[2] Max S. Zolotorev,[3] Hidekazu Mimura,[4] Hirokatsu Yumoto,[4] Satoshi Matsuyama,[4] Kazuto Yamauchi,[4] and Tetsuya Ishikawa[1,5]

[1]*SPring-8/JASRI, Kouto 1-1-1, Sayo, Hyogo 679-5198, Japan*

[2]*Stanford Synchrotron Radiation Laboratory/SLAC, Menlo Park, California 94025, USA*

[3]*Center for Beam Physics, Accelerator and Fusion Research Division, Lawrence Berkeley National Laboratory, University of California, Berkeley, California 94720, USA*

[4]*Department of Precision Science and Technology, Graduate School of Engineering, University of Osaka, 2-1 Yamada-oka, Suita, Osaka 565-0871, Japan*

[5]*SPring-8/RIKEN, Kouto 1-1-1, Sayo, Hyogo 679-5148, Japan*

(Received 24 May 2006; published 25 August 2006)

An experimental scheme to realize single-shot spectrometry for the diagnostics of x-ray free-electron lasers (XFELs) is presented. The combination of an ultraprecisely figured mirror and a perfect crystal form a simple, high-precision spectrometer that can cover an energy range from a few eV to a hundred eV with high resolution. The application of the spectrometer to determine XFEL pulse widths was investigated theoretically and experimentally. It has been shown that the present system can determine pulse widths from sub-fs to ps in a single shot even for spontaneous radiation. The system can be easily extended to even shorter pulses.

DOI: 10.1103/PhysRevLett.97.084802 PACS numbers: 41.50.+h, 07.85.Qe, 42.50.Ar

X-ray free-electron lasers (XFELs) will provide novel insights into atomic-scale science with ultrafast time resolution. The XFELs currently proposed [1–3] are based on the self-amplified spontaneous emission (SASE) principle [4], which combines a long undulator with a linac. Because shot-to-shot variations of linac beam parameters can be large, single-shot diagnostics of the electron and photon beams are crucial for realizing stable FEL saturation. Naturally, the photon beam diagnostics give essential information for all XFEL applications. In particular, precise evaluation of the x-ray pulse width is a critical issue for many experiments such as ultrafast chemistry, nonlinear optics, and single molecular diffraction [5].

The photon beam is characterized by a density in six-dimensional (6D) phase space (i.e., energy time and a couple of spatial-momentum coordinates) with polarization information. One of the most important targets in XFEL diagnostics is the single-shot measurement of the energy spectrum. A straightforward application with moderate resolution ($\Delta E/E \geq 10^{-4}$) is to trace photon beam energy with every shot, which leads to precise evaluation of the electron beam energy. This is also useful for characterizing magnetic fields of undulators.

Higher-resolution measurements ($\Delta E/E < 10^{-4}$) enable one to resolve the microstructure of the energy spikes that originate from the random superposition of coherent wave packets. This is very attractive because the structure gives a clue for the simple determination of the pulse width. Furthermore, the statistical analysis of the structure gives the second-order coherence properties of radiation [6]. The principle is based on the fact that the microstructure in the energy domain is related to the macrostructure (envelope) in the temporal domain by a Fourier transform [7–10]. If we denote their averaged widths as $\Delta E$ and $\Delta t$ (in FWHM), the product $\Delta E \Delta t$ is simply equal to 1.8 eV · fs for Gaussian distributions.

In synchrotron radiation, single-shot spectrum measurements with Fourier-limited resolution have been realized for low-energy photon beams. Sugahara *et al.* developed a single-shot spectrometer for THz coherent radiation from short-bunched electrons bent in a dipole magnet [11]. Catravas *et al.* measured the microstructure of the energy spectrum of visible light from a wiggler installed in a linac [10]. Recently, a group at the TESLA Test Facility (TTF) has succeeded in measuring the vacuum ultraviolet (VUV) spectrum of SASE-FEL by single-shot detection [12]. For evaluating pulse widths, these ''energy-domain'' methods are complementary to the ''time-domain'' methods such as the correlation method using an external laser [13]. Notable features of the former are as follows: (i) the measurement is free from the timing jitter between the x rays and the external trigger, and (ii) the required spectral resolution of the analyzer system becomes relaxed as the pulse width decreases owing to their reciprocal relationship. The method can therefore be applied to the evaluation of pulse widths shorter than a femtosecond.

In the x-ray region, high-resolution spectrometry with sub-meV resolution is realized using crystal monochromators [14,15] or analyzers [16]. However, they are in general not designed for single-shot measurements. Although a dispersive spectrometer which combines a curved crystal with an array detector [17] can realize single-shot measurements, the achieved bandwidth of ~1 eV, which is mainly limited by the lattice distortion of the bent crystal, is insufficient for resolving energy spikes originating from pulse lengths ≥ 100 fs. In this Letter, we present a simple scheme for realizing both high-resolution and single-shot spectrometry for the diagnostics of XFEL. We demon-

 

strated the validity of the method by performing a proof-of-principle experiment. We focus on the application for the evaluation of XFEL pulse widths by this method.

Figure 1 shows a schematic of the experimental setup used at the 1 km beam line of SPring-8 [18]. The nearly parallel incident x rays ($E = 10$ keV, angular divergence $\Omega_i = 0.3$ $\mu$rad) are converted to the divergent beam (divergence $\Omega_o = 2.3$ mrad) by an elliptical mirror, which is made from single-crystal silicon with a Pt-coated surface. The smoothness of mirror surface is very important for reducing unwanted intensity variations, referred to as speckles [19]. Thus, the surface is ultraprecisely figured by the combination of elastic emission machining (EEM) [20] and microstitching interferometry (MSI) [21]. The divergent beam is dispersed with a flat analyzer crystal using the Si 555 symmetric reflection. The Bragg angle is $\theta_B = 81.3°$ for $E = 10$ keV. The analyzed beam is then detected with a position sensitive device. At the detector plane set normal to the beam, the lateral shift $\Delta d$ of the dispersed beam with energy deviation $\Delta\epsilon$ is given by

$$\Delta d = \frac{\Delta\epsilon}{E} L \tan\theta_B, \tag{1}$$

where $L$ is the distance between the focal point to the detector.

Although our final goal is single-shot detection, the photon flux in the present synchrotron light source is insufficient for the purpose. To study a fundamental property of the scheme, we set a Si 555 channel-cut monochromator with a narrow bandpass of $\Delta E_M = 13.8$ meV. The energy deviation $\Delta\epsilon$ is controlled by angular tuning of the monochromator. Figure 2(a) shows images of the dispersed beam detected with a CCD (pixel size of 6 $\mu$m $\times$ 6 $\mu$m, 1024 $\times$ 1024 pixels). The beam position shifts as the monochromatic photon energy changes. For finer spatial resolution measurements, a gold wire (diameter of 100 $\mu$m) placed in front of an avalanche photodiode (APD) was scanned at 2.5 $\mu$m steps. In Fig. 2(b), deviations of the central positions $\Delta d$ are plotted as a function of photon energy. The line is a fit to Eq. (1) with a fitting parameter $L = 1.71$ m, which agreed with the experimental setup. The differences from the linear fit $\Delta d - \Delta d_{\rm fit}$ (shown as open circles in the figure) are smaller than 4 $\mu$m.

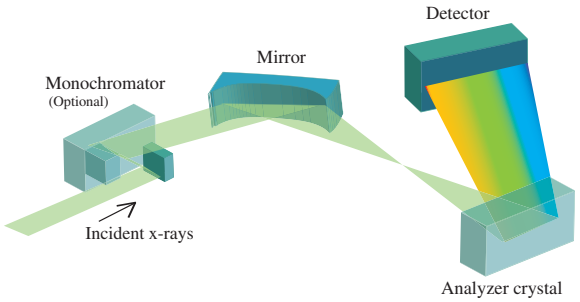


FIG. 1 (color online). Schematic view of experimental setup. The incident beam is diverged by the mirror and dispersed by the analyzer crystal. The detector measures the energy spectrum as a spatial intensity distribution. The monochromator is used for evaluating the performance of the system.

We studied the energy resolution achieved with this system. Figure 3 shows a typical profile of the dispersed beam measured by scanning the Au wire. The average beamwidth is determined to be $21.3 \pm 3.1$ $\mu$m, which corresponds to an overall energy bandwidth of $\Delta E_T = 19.0 \pm 2.7$ meV with Eq. (1). The intrinsic bandwidth of the analyzing system is $\Delta E = \sqrt{\Delta E_T^2 - \Delta E_M^2} = 13.1 \pm 1.9$ meV. Theoretically, we evaluate the value on the basis of spherical-wave diffraction theory [22]. The resolution is

$$\frac{\Delta E}{E} = \frac{\cot\theta_B \sqrt{\sigma_x^2 + (2p\Lambda\cos\theta_B)^2 + \omega_s^2 L'^2}}{L}, \tag{2}$$

where $\sigma_x$ is the focal size of the mirror, $L'$ is the distance from the crystal to the detector, $p$ is a dimensionless coefficient (we set $p = 1.6$, as obtained from the numerical calculation), and $\omega_s$ and $\Lambda$ are the total reflection width and the extinction distance of the analyzer crystal, respectively. Applying our parameters $\sigma_x = 1.4$ $\mu$m, $L' = 0.79$ m, $\omega_s = 8.63$ $\mu$rad, and $\Lambda = 30.2$ $\mu$m, the theoretical bandwidth is determined to be $\Delta E = 14.5$ meV, which is in good agreement with the experiment.

The energy resolution is related to the maximum pulse width that can be determined. Below we give a theoretical explanation. We suppose that light to the detector is transversely coherent and is chaotic longitudinally. Then the enhancement of the normalized intensity correlation function in the frequency domain is given by [7]

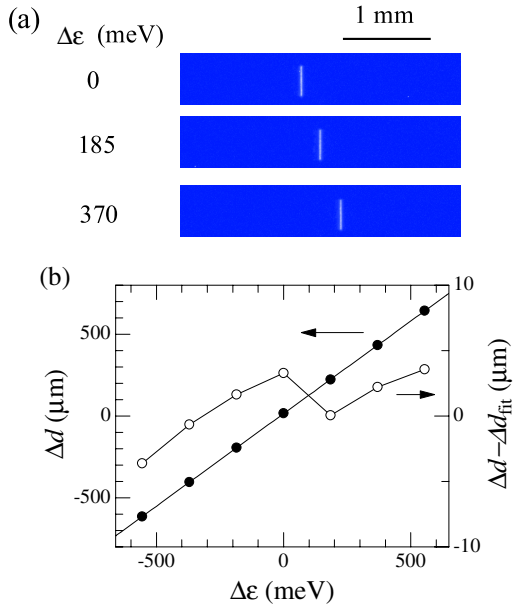


FIG. 2 (color online). (a) CCD images of dispersed beams for different incident energies. (b) Positional dependence of dispersed beam on beam energy $\Delta\epsilon$. The solid circles (corresponding to the left axis) show the position $\Delta d$, while the open circles (corresponding to the right axis) indicate the difference $\Delta d - \Delta d_{\rm fit}$.

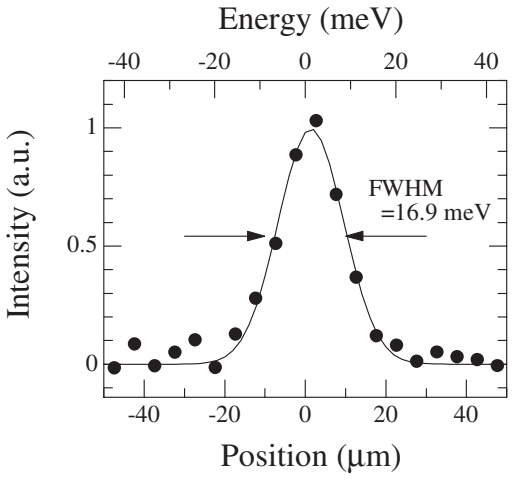


FIG. 3. Spatial profile of dispersed beam (lower axis). The corresponding energy scale is shown on the upper axis.

$$\hat{C}_I(\Delta\omega) = \langle I(\omega)I(\omega+\Delta\omega)\rangle/|\langle I(\omega)\rangle|^2 - 1 = |\gamma(\Delta\omega)|^2, \tag{3}$$

where $\langle\cdots\rangle$ is the average over the frequency, and $\gamma(\Delta\omega)$ is the first-order coherence function. In fact, the finite energy bandwidth of the measurement system should be taken into account. The function is then modified as

$$\hat{C}_F(\Delta\omega) = \int_{-\infty}^{\infty} da \int_{-\infty}^{\infty} da' R(a)R(a')|\gamma(\Delta\omega - a' + a)|^2, \tag{4}$$

where $R(a)$ corresponds to the resolution function of the analyzing system. For simplicity, we suppose that the coherence and the resolution functions are the Gaussian distributions with rms widths of $\sigma_c$ $(=2\sqrt{2\ln 2}/\Delta t)$ and $\sigma_r$ $(=\Delta E/2\hbar\sqrt{2\ln 2})$, respectively. Then Eq. (4) is reduced to

$$\hat{C}_F(\Delta\omega) = \frac{\sigma_c}{\sqrt{\sigma_c^2 + 4\sigma_r^2}} \exp\left(-\frac{\Delta\omega^2}{\sigma_c^2 + 4\sigma_r^2}\right) \equiv \hat{C}_{\max} \exp\left(-\frac{\Delta\omega^2}{\sigma_T^2}\right). \tag{5}$$

The term $\sigma_c$, which is related to the pulse width $\Delta t$, can be retrieved from the maximum enhancement $\hat{C}_{\max}$ [10]. The correlation width $\sigma_T$ becomes another good reference for evaluating $\Delta t$, if the condition $\hat{C}_{\max} \simeq 1$ is required. We investigate the dependence of $\hat{C}_{\max}$ on $\Delta t$ for several bandwidths $\Delta E$. The result, which is shown in Fig. 4, indicates that an appropriate choice of $\Delta E$ permits the determination of $\Delta t$ over a wide range.

In particular, the bandwidth $\Delta E = 13.1$ meV in the present setup covers the range $\Delta t \leq 10$ ps. The noise in the real measurement, however, can raise the minimum detection level of $\hat{C}_{\max}$, and suppress the upper limit of determinable pulse width. It is considered that the most serious noise from the optical components is the speckles in the mirror reflection; the angular intensity modulation of the reflected beam causes intensity variations in the final energy spectrum. We measured intensity distributions by scanning the incident energy $\Delta\epsilon$ for different illuminated mirror areas: the EEM-finished and prefinished parts. The standard deviations, $\sigma_I$, of the fluctuation are measured to be 0.079 and 0.35, respectively. We found that the fluctuation is much reduced under the former condition. If we regard the fluctuation levels as the minimum detectable values of $\hat{C}_{\max}$, the maximum pulse widths to be determined are 1.8 and 0.4 ps, respectively, as seen in Fig. 4. The result shows that high-quality mirror surfaces are essential for determining pulse widths in the sub-ps to ps region.

Next, we consider the minimum measurement limit of the pulse width. In this case, we assume that $\hat{C}_{\max} \simeq 1$ is required and that the pulse width is evaluated from the width $\sigma_T$. Because $\sigma_T$ increases as $\Delta t$ decreases, the minimum detection limit of $\Delta t$ is related to the total energy range $\Delta E_w$ of the analyzer system, which is given by

$$\Delta E_w = E\Omega_o \cot\theta_B. \tag{6}$$

The value is $\Delta E_w = 3.5$ eV with the present parameters, which corresponds to a single-mode pulse width of $\Delta t = 520$ as. For much shorter pulses, we can switch the reflecting plane of the analyzer crystal to a lower index. For example, the use of the Si 111 reflection ($\theta_B = 11.4°$ at $E = 10$ keV) gives $\Delta E_w = 114.1$ eV, which corresponds to a width of $\Delta t = 16$ as.

Finally, we evaluate the statistical noise of $\hat{C}_{\max}$ involved in photon detection. In the photon counting scheme, the enhancement $\hat{C}_{\max}$ is connected to the counting number $K$ in a detector pixel [7],

$$\hat{C}_{\max} = \frac{\langle K^2\rangle - \langle K\rangle^2 - \langle K\rangle}{\langle K\rangle^2}. \tag{7}$$

The signal-to-noise ratio, SNR $= \hat{C}_{\max}/\Delta\hat{C}_{\max}$, can be ob-

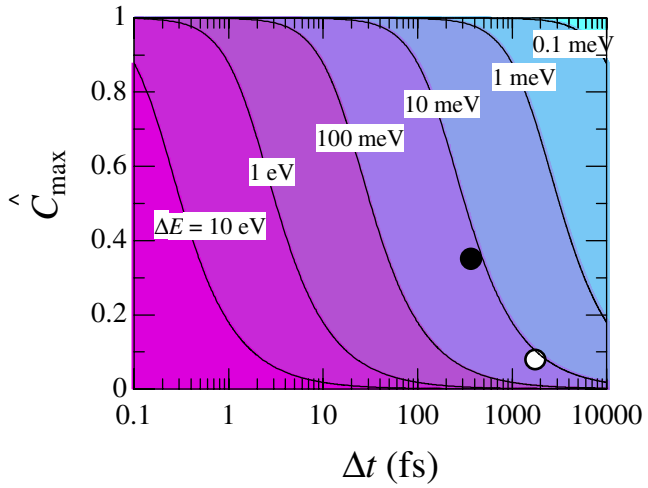


FIG. 4 (color online). Maximum enhancement $\hat{C}_{\max}$ as a function of $\Delta t$. The parameter is the bandwidth $\Delta E$. The solid (open) circle shows the measured intensity fluctuation $\sigma_I$ on the contour line $\Delta E = 13.1$ meV for the EEM-finished (prefinished) part of the mirror.

tained by calculating the second-order moment of $\hat{C}_{\max}$. Assuming that the pixel number $N_p$ is large, SNR can be represented as [23]

$$\mathrm{SNR} = p\sqrt{N_p/2} \times [(1 + M^{-1}) + 2p(1 + 2M^{-1}) + p^2(1 + 3M^{-1})]^{-1/2}, \quad (8)$$

where $p = \langle K \rangle / M$ and $M$ is the mode number, which is equal to the reciprocal of $\hat{C}_{\max}$. We investigate Eq. (8) in two limiting cases. If the photon number in a single mode is small, i.e., $p \ll 1$, SNR converges to $p\sqrt{N_p/2}$, which is a form similar to that of intensity interferometry based on the coincidence technique [7,24]. In contrast, the SNR approaches $\sqrt{N_p/[2(1 + 3/M)]}$ when $p \gg 1$. This is independent of $p$ because the effect of the Bose-Einstein statistics that have large fluctuations becomes significant in this case. With the present optics, $p$ is represented as

$$p \simeq \frac{\alpha \delta_D}{N_p} \sqrt{1 - 1/M^2}, \quad (9)$$

where $\alpha$ and $\delta_D$ are the efficiency and the Bose degeneracy, respectively. Note that $N_p$ in the denominator is due to the dispersive optical arrangement. Now we evaluate SNR using the photon beam parameters given in Ref. [2]. For the present optics with $\Delta t = 200$ fs, $\alpha = 0.8$, and $M = 1.7$ is obtained. The degeneracy is expected from $\delta_D \sim 10^3$ (for spontaneous radiation) to $\delta_D \sim 10^8$ (for the SASE saturated condition). In the former case, $p \simeq 1$ is obtained from Eq. (9) by setting the detector pixel number $N_p = 10^3$. Then a SNR $\simeq 7.6$ is determined from Eq. (8). The value corresponds to an error of $\Delta t$ to be 40 fs, from an analysis based on Fig. 4. The result shows that single-shot detection is plausible even for spontaneous radiation. For a saturated SASE beam, $p$ is a large number and one is able to analyze the original correlation function $\hat{C}_F(\Delta\omega)$ with a good statistics, which provides more detailed information about the pulse shape and statistical properties of the photon beam.

In conclusion, we presented a simple scheme for single-shot spectrometry of XFEL. An energy range from a few eV to a hundred eV can be selected by choosing an appropriate reflecting plane of the analyzer crystal. The application of the method to evaluation of pulse width was discussed. The maximum measurement limit is determined by the energy resolution and the uniformity of the intensity distribution, while the minimum limit is dominated by the energy range. The present optics with the Si 555 reflection can cover a wide temporal range, 520 as $\leq \Delta t \leq 1.6$ ps. Much shorter times are easily achieved by changing the reflecting plane to a lower index. The method can trace a change in temporal profile through the evolution of the lasing process from the exponential growth regime to saturation, which will provide important experimental information on the SASE lasing mechanism. The measurement can also reveal the second-order coherence of the light source. This is necessary for understanding the radiation properties of future XFELs, which aim at single-mode lasing [25–27].

One of the authors (M. Y.) thanks Dr. S. Goto and Dr. H. Yamazaki for fruitful discussions on the spherical-wave diffraction theory. This research was partially supported by MEXT through a Grant in Aid for Young Scientists, No. 17760062.

*Electronic address: yabashi@spring8.or.jp

[1] *SCSS X-FEL Conceptual Design Report*, RIKEN Harima Institute, Sayo, Japan, 2005.
[2] Stanford Linear Accelerator Center Report No. SLAC-R-521, 1998.
[3] Deutsches Elektronen Synchrotron Report No. DESY97-048, edited by R. Brinkmann, G. Materlik, J. Rossbach, and A. Wagner, 1997.
[4] R. Bonifacio, C. Pellegrini, and L. Narducci, Opt. Commun. **50**, 373 (1984).
[5] R. Neutze, R. Wouts, D. van der Spoel, E. Weckert, and J. Hajdu, Nature (London) **406**, 752 (2000).
[6] E. L. Saldin, E. A. Schneidmiller, and M. V. Yurkov, *The Physics of Free Electron Lasers* (Springer, New York, 1999).
[7] J. W. Goodman, *Statistical Optics* (Wiley, New York, 1985).
[8] M. S. Zolotorev and G. V. Stupakov, SLAC Report No. SLAC-PUB-7132, 1996.
[9] J. Krzywinski, E. L. Saldin, E. A. Schneidmiller, and M. V. Yurkov, Nucl. Instrum. Methods Phys. Res., Sect. A **401**, 429 (1997).
[10] P. Catravas *et al.*, Phys. Rev. Lett. **82**, 5261 (1999).
[11] J. Sugahara *et al.*, in *Proceedings of the 1999 Particle Accelerator Conference* (IEEE, New York, 1999), Vol. 4500, p. 2187.
[12] V. Ayvazyan *et al.*, Phys. Rev. Lett. **88**, 104802 (2002).
[13] A. L. Cavalieri *et al.*, Phys. Rev. Lett. **94**, 114801 (2005).
[14] M. Yabashi, K. Tamasaku, S. Kikuta, and T. Ishikawa, Rev. Sci. Instrum. **72**, 4080 (2001).
[15] M. Yabashi, K. Tamasaku, and T. Ishikawa, Phys. Rev. Lett. **87**, 140801 (2001).
[16] R. Verbeni *et al.*, J. Synchrotron Radiat. **3**, 62 (1996).
[17] T. Matsushita and R. Phizackerley, Jpn. J. Appl. Phys. **20**, 2223 (1981).
[18] T. Ishikawa *et al.*, Proc. SPIE-Int. Soc. Opt. Eng. **4145**, 1 (2001).
[19] H. Mimura *et al.*, J. Synchrotron Radiat. **11**, 343 (2004).
[20] Y. Mori *et al.*, Proc. SPIE-Int. Soc. Opt. Eng. **4501**, 30 (2001).
[21] K. Yamauchi *et al.*, Rev. Sci. Instrum. **74**, 2894 (2003).
[22] T. Saka, T. Katagawa, and N. Kato, Acta Crystallogr. Sect. A **29**, 192 (1973).
[23] M. R. Spiegel, *Theory and Problems of Probability and Statistics* (McGraw-Hill, New York, 2000).
[24] E. Ikonen, Phys. Rev. Lett. **68**, 2759 (1992).
[25] J. Feldhaus *et al.*, Opt. Commun. **140**, 341 (1997).
[26] L. H. Yu *et al.*, Science **289**, 932 (2000).
[27] P. Emma *et al.*, Phys. Rev. Lett. **92**, 074801 (2004).